Letter

# Luttinger-compensated bipolarized magnetic semiconductor

Peng-Jie Guo,[1,2,*] Huan-Cheng Yang,[1,2] Xiao-Yao Hou,[1,2] Ze-Feng Gao,[1,2] Wei Ji,[1,2,†] and Zhong-Yi Lu[1,2,3,‡]

[1]*Department of Physics and Beijing Key Laboratory of Opto-electronic Functional Materials & Micro-nano Devices, Renmin University of China, Beijing 100872, China*

[2]*Key Laboratory of Quantum State Construction and Manipulation (Ministry of Education), Renmin University of China, Beijing 100872, China*

[3]*Hefei National Laboratory, Hefei 230088, China*

(Received 25 February 2025; revised 23 May 2025; accepted 27 October 2025; published 13 November 2025)

Altermagnetic materials, with real-space antiferromagnetic arrangement and reciprocal-space anisotropic spin splitting, have attracted much attention. However, the spin splitting is small in most altermagnetic materials, which is a disadvantage to their application in electronic devices. In this study, based on symmetry analysis and the first-principles electronic structure calculations, we predict two Luttinger compensated bipolarized magnetic semiconductors $Mn(CN)_2$ and $Co(CN)_2$ with *s*-wave spin splitting as in the ferromagnetic materials. Our further analysis shows that the Luttinger compensated magnetism here depends not only on spin group symmetry, but also on the crystal field splitting and the number of *d*-orbital electrons. In addition, the polarized charge density indicates that both $Mn(CN)_2$ and $Co(CN)_2$ have the quasisymmetry $T\tau$, resulting from the crystal field splitting and the number of *d*-orbital electrons. The Luttinger compensated magnetism not only has the zero total magnetic moment as the antiferromagnetism, but also has the *s*-wave spin splitting as the ferromagnetism, thus our work not only provides theoretical guidance for searching Luttinger compensated magnetic materials with distinctive properties, but also provides a material basis for the application in spintronic devices.

DOI: 10.1103/9syc-71w8

*Introduction.* Ferromagnetic (FM) semiconductors with spintronic and transistor functionalities have strongly attracted experimental and theoretical interest due to their potential applications in next-generation electronic devices [1–5]. However, ferromagnetic materials are usually more likely to be metals than insulators. Although many ferromagnetic semiconductors have been proposed [6–11], their magnetic transition temperatures are relatively low, which hinders their application in electronic devices. In addition, there are another two shortcomings. First, a key disadvantage of ferromagnetic semiconductors is the effect of stray fields due to nonzero net magnetic moments. Second, the slow reversal of ferromagnetic domain is not conducive to the improvement of device speed. Compared with ferromagnetic materials, antiferromagnetic materials are usually insulators very likely with high Néel temperatures, and may take the advantages of feasible miniaturization due to zero total magnetic moments and fast domain reversal speed. An interesting question is whether or not there are magnetic materials that simultaneously share the respective excellent features of ferromagnetic semiconductors and antiferromagnetic insulators.

Recently, based on spin group theory, altermagnetism distinct from ferromagnetism and conventional antiferromagnetism has been proposed [12,13]. Interestingly, altermagnetic materials may simultaneously share the respective excellent features of ferromagnetic materials and antiferromagnetic materials but without their disadvantages. Thus, altermagnetic materials show many novel physical properties [12–42]. In altermagnetism, opposite spin lattices cannot be connected by space-inversion symmetry $\{C_2||I\}$ or fractional translation symmetry $\{C_2||\tau\}$, but by rotation or mirror symmetry $\{C_2||R\}$. Here, the symmetry operations at the left and right of the double vertical bar act only on the spin space and lattice space, respectively; the notation $C_2$ represents the 180° rotation perpendicular to the spin direction; the notations $I$, $R$, and $\tau$ denote space inversion, rotation/mirror, and fractional translation operations, respectively. The spin symmetry $\{C_2||R\}$ guarantees zero total magnetic moment, while the breaking of the spin symmetry $\{C_2||I\}$ and $\{C_2||\tau\}$ leads to altermagnetic materials with anisotropic spin splitting, such as *d*-wave, *g*-wave, and *i*-wave spin splitting. The anisotropic spin splitting in altermagnetic materials differs from the *s*-wave spin splitting in ferromagnetic materials. It thus raises an interesting question: does a magnetic phase exist that exhibits both isotropic spin splitting and net zero total magnetic moment?

Inspired by the definition of altermagnetism, we consider such a magnetic phase in which the opposite spin lattices cannot be connected by any crystal symmetry, but the total magnetic moment in the unit cell is exactly zero. When a material is an insulator or half-metal, the spin magnetic moments per unit cell can have only integer value in Bohr magnetons by Luttinger's theorem [43,44]. Consequently, if the total spin magnetic moment of the material is relatively small, it will be exactly zero. Further, if the orbital magnetic moments of the material is simultaneously completely quenched in the crystal field, its total magnetic moment will be zero. This magnetic phase is named as Luttinger

*Contact author: guopengjie@ruc.edu.cn
†Contact author: wji@ruc.edu.cn
‡Contact author: zlu@ruc.edu.cn

 

compensated magnetic phase [18]. Different from altermagentic materials, the Luttinger compensated magnetic materials have *s*-wave spin polarization, which is similar to ferromagnetic materials and beneficial to improve the spin polarization of carriers. Thus, the Luttinger compensated magnetism may simultaneously also take the respective advantage of ferromagnetism and antiferromagnetism. Moreover, considering that the Luttinger compensation magnetism generally has an *s*-wave spin splitting and completely polarized carriers, it may have more advantages than altermagnetism in electronic device applications. Although a minority of materials have been theoretically predicted to be of this type of compensated magnetic materials [16,45–49], it is very important for the research of Luttinger compensated magnetism to predict more candidate materials.

In this study, we predict two Luttinger compensated bipolarized magnetic semiconductors $Mn(CN)_2$ and $Co(CN)_2$, whose opposite spin lattices cannot be connected by any crystal symmetry but with fully compensated total magnetic moments. Moreover, the polarized charge density indicates that both $Mn(CN)_2$ and $Co(CN)_2$ have the quasisymmetry $T\tau$, resulting from the crystal field splitting and the number of *d*-orbital electrons. Finally, we propose a scheme to search for the Luttinger compensated magnetic materials.

*Method.* Our electronic structure calculations employed the Vienna *ab initio* simulation package (VASP) [50] with the projector augmented wave (PAW) method [51]. The Perdew-Burke-Ernzerhof (PBE) exchange-correlation functional [52] and the GGA plus on-site repulsion $U$ method (GGA + $U$) were used in our calculations [53,54]. The kinetic energy cutoff was set to be 600 eV for the expanding of the wave functions into a plane-wave basis and the energy convergence criterion is $10^{-6}$ eV. The Γ-centered $k$ mesh was set as $12 \times 12 \times 12$. The crystal structures were fully relaxed until the force on each atom is less than 0.01 eV/Å. The relaxed lattice parameters were 6.04 Å and 5.75 Å for $Co(CN)_2$ and $Mn(CN)_2$, respectively. The Monte Carlo simulations based on the classical Heisenberg model were performed by using the open source project MCSOLVER [55].

*Results and discussion.* Based on spin space symmetry, collinear compensated magnetism can be divided into three categories. The first category is conventional collinear antiferromagnetism, where opposite spin sublattices are connected by spin symmetry $\{C_2||I\}$ or $\{C_2||\tau\}$. Without spin-orbit coupling (SOC), bands are always spin degenerate in conventional collinear antiferromagnetic materials. When SOC is considered, spin symmetries $\{C_2||I\}$ or $\{C_2||\tau\}$ transform into $IT$ and $T\tau$ symmetries, respectively. Conventional collinear antiferromagnetic materials with $IT$ symmetry remain spin degenerate, while those with $T\tau$ symmetry exhibit spin splitting induced by SOC. The second category is altermagnetism, where opposite spin sublattices are connected by spin symmetry $\{C_2||R\}$. Altermagnetic materials exhibit anisotropic spin splitting without SOC. With SOC, spin-degenerate bands at high-symmetry planes or lines may split, depending on the symmetry. The third category is Luttinger compensated magnetism, where opposite spin sublattices cannot be connected by any symmetry. Luttinger compensated magnetic materials exhibit *s*-wave spin splitting without SOC.

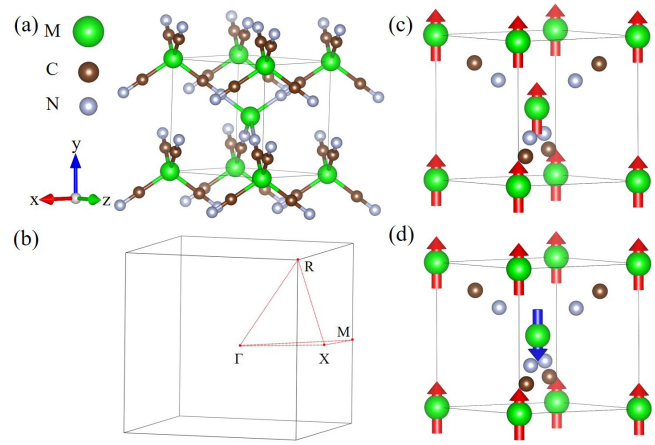


FIG. 1. The crystal structure and two typical magnetic structure of $M(CN)_2$. (a) and (b) are the crystal structure and Brillouin zone (BZ) of $M(CN)_2$. The red points represent high-symmetry points. Two typical collinear magnetic configurations of $M(CN)_2$: (c) the FM state and (d) the AFM state. The red and blue arrows represent the up and down spin moments, respectively.

For Luttinger compensated magnetic materials, the opposite spin sublattices need to have different crystal field environments to guarantee that they cannot be connected by any crystal symmetry. Here, we propose a cubic crystal structure $M$ ($M$ = Mn and Co) $(CN)_2$, in which two magnetic atoms $M$ are surrounded by regular tetrahedra of C and N [Fig. 1(a)], respectively. Therefore, $M(CN)_2$ has P-43m (215) space group symmetry without space-inversion symmetry, and the corresponding point group symmetry is $T_d$. The Brillouin zone (BZ) of $M(CN)_2$ with high-symmetry lines and points is shown in Fig. 1(b). To determine the magnetic structure of $M(CN)_2$, we consider two magnetic structures: ferromagnetic and antiferromagnetic, which are shown in Figs. 1(c) and 1(d), respectively. We calculated the total energies of two magnetic structures for $Mn(CN)_2$ and $Co(CN)_2$ with the variation of Hubbard interaction $U$, which are shown in Figs. 2(a) and 2(c), respectively. From Figs. 2(a) and 2(c), the antiferromagnetic state is always stable under different Hubbard interaction $U$ for both $Mn(CN)_2$ and $Co(CN)_2$. On the other hand, since the angle between $M$-CN-$M$ is of 180°, $M$-$M$ favors antiferromagnetic coupling according to GKA rules [56]. Therefore, the results of electronic structure calculations and theoretical analysis are consistent.

Due to the absence of space-inversion symmetry, $M(CN)_2$ has no $\{C_2||I\}$ symmetry. At the same time, $M(CN)_2$ has no $\{C_2||\tau\}$ symmetry due to the presence of C and N atoms in crystal cell. So both $Mn(CN)_2$ and $Co(CN)_2$ are not conventional collinear antiferromagnetic materials. Although the $T_d$ group has 24 symmetric operations including E, $8C_3$, $3C_2$, $6\sigma_d$, and $6S_4$, none of them can connect the spin opposite magnetic atoms $M$ in $M(CN)_2$. Therefore, both $Mn(CN)_2$ and $Co(CN)_2$ are not altermagnetic materials either, but may be Luttinger compensated magnetic materials. On the other hand, we also calculated the phonon spectra of $Mn(CN)_2$ and $Co(CN)_2$, which are shown in Figs. 2(b) and 2(d), respectively, to check their dynamical stability. From Figs. 2(b) and 2(d), neither $Mn(CN)_2$ nor $Co(CN)_2$ has imaginary

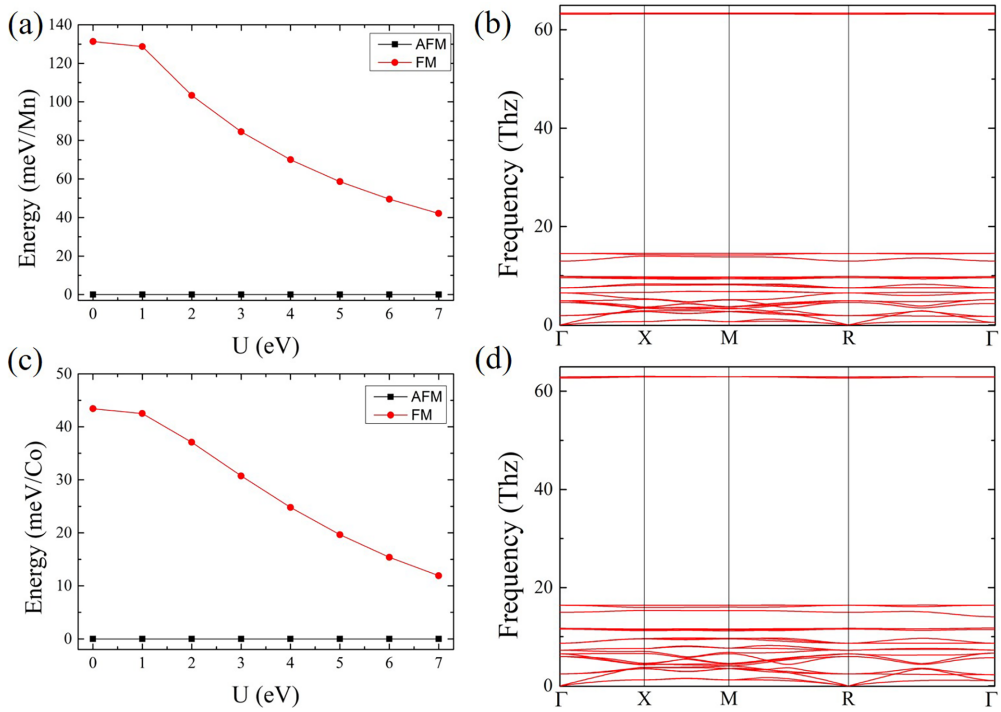


FIG. 2. Relative energy of different magnetic structures with variation of Hubbard interaction $U$ and phonon spectra for $M(CN)_2$. (a) and (c) are relative energies of AFM state with respect to the FM state for $Mn(CN)_2$ and $Co(CN)_2$, respectively. (b) and (d) are the phonon spectrum of $Mn(CN)_2$ and $Co(CN)_2$, respectively.

frequencies in their phonon spectra. Thus, $Mn(CN)_2$ and $Co(CN)_2$ are dynamically stable.

After verifying the structural stability and magnetic structure, we next study the electronic properties of $Mn(CN)_2$ and $Co(CN)_2$. Without spin-orbit coupling (SOC), both $Mn(CN)_2$ and $Co(CN)_2$ are semiconductors with bandgaps to be 3.89 eV and 2.4 eV as shown in Figs. 3(a) and 3(b), respectively. Different from altermagnetic materials, their spin-up and spin-down bands are completely split, and the spin splitting of conduction bands for both $Mn(CN)_2$ and $Co(CN)_2$ is greater than 500 meV [Figs. 3(a) and 3(b)]. This is because atoms with opposite magnetic moments cannot be connected by any symmetry. But, the total magnetic moments of both $Mn(CN)_2$ and $Co(CN)_2$ are zero, which is the same as those of altermagnetic and conventional collinear antiferromagnetic materials. Interestingly, the highest occupied valence band and the lowest unoccupied conduction band have opposite spin polarizations for both $Mn(CN)_2$ and $Co(CN)_2$ [Figs. 3(a) and 3(b)], thus both $Mn(CN)_2$ and $Co(CN)_2$ are bipolarized magnetic semiconductors.

On the other hand, the magnetic transition temperature is very important for the application of magnetic materials. We estimated the magnetic transition temperatures $T_N$ of $Mn(CN)_2$ and $Co(CN)_2$ from the classical Monte Carlo simulations based on the three-dimensional lattice Heisenberg model. The Hamiltonian is shown as follows:

$$H = J_1 \sum_{i,j} S_i \cdot S_j, \tag{1}$$

where $S_i$ represents the spin of Co or Mn on site $i$ and $J_1$ denotes the first-nearest neighbor exchange interaction parameters. The exchange interaction parameters were derived from mapping the energies of the FM and AFM magnetic configurations to the above model. The results are $J_1S^2 = 3.10$ and 8.75 meV for $Co(CN)_2$ and $Mn(CN)_2$, respectively. Then, the magnetic transition temperatures can be extracted from the peak of the specific-heat capacity based on the Monte Carlo simulations. As shown in Figs. 4(a) and 4(b), the resultant magnetic transition temperatures for $Mn(CN)_2$ and $Co(CN)_2$ are 210 K and 75 K, respectively.

An important question is why both $Mn(CN)_2$ and $Co(CN)_2$ have exactly zero total magnetic moments. The question may be answered by the following three points. First, in the crystal of $M(CN)_2$, the $Mn^{+2}$ and $Co^{+2}$ ions are located in the regular tetrahedral crystal field. Therefore, the $3d$ orbits will split into $E_g$ and $T_{2g}$ orbits, and the $E_g$ orbits has lower energy than the $T_{2g}$ orbits as shown in Fig. 4(c). The $Mn^{+2}$ and $Co^{+2}$ ions have five and seven $d$ electrons, respectively. In the high-spin state, the orbital magnetic moments of both $Mn^{+2}$ and $Co^{+2}$ ions are completely quenched and the magnetic moments can only arise from spin moments. Second, both $Mn(CN)_2$ and $Co(CN)_2$ are insulators, which requires that they can have only an integer spin magnetic moment in Bohr magnetons per unit cell by Luttinger's theorem [43,44]. Finally, the opposite spin magnetic moments on $Mn^{+2}$ ($Co^{+2}$) in $Mn(CN)_2$ [$Co(CN)_2$] are almost equal in size, then the total spin magnetic moment in the unit cell should be very samll and it will then be exactly zero due to the constraint of Luttinger's theorem [43,44]. On the other hand, we also calculated the polarized charge densities of $Mn(CN)_2$ and $Co(CN)_2$, which are shown in Figs. 3(b) and 3(d), respectively. From Figs. 3(b) and 3(d), the polarized charge density distribution of two $Mn^{+2}$

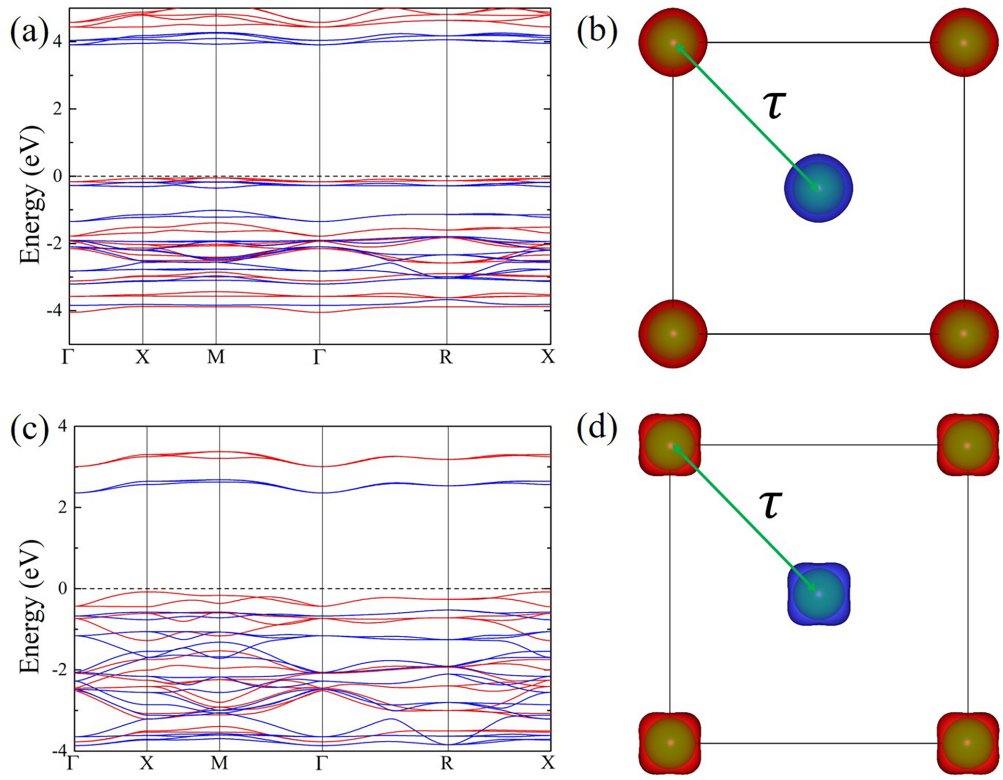


FIG. 3. The electronic band structure and polarized charge density of $M(CN)_2$. (a) and (c) are the electronic band structures of $Mn(CN)_2$ and $Co(CN)_2$ along the high-symmetry directions, respectively. The red and blue lines represent spin-up and spin-down channels, respectively. The polarized charge density of $Mn(CN)_2$ (b) and $Co(CN)_2$ (d). The red and blue three-dimensional surface represent, respectively, spin-up and spin-down polarized charge density. The $\tau$ represents (1/2, 1/2, 1/2) fractional translation. The electronic structure and polarized charge density are calculated with $U = 4$ eV.

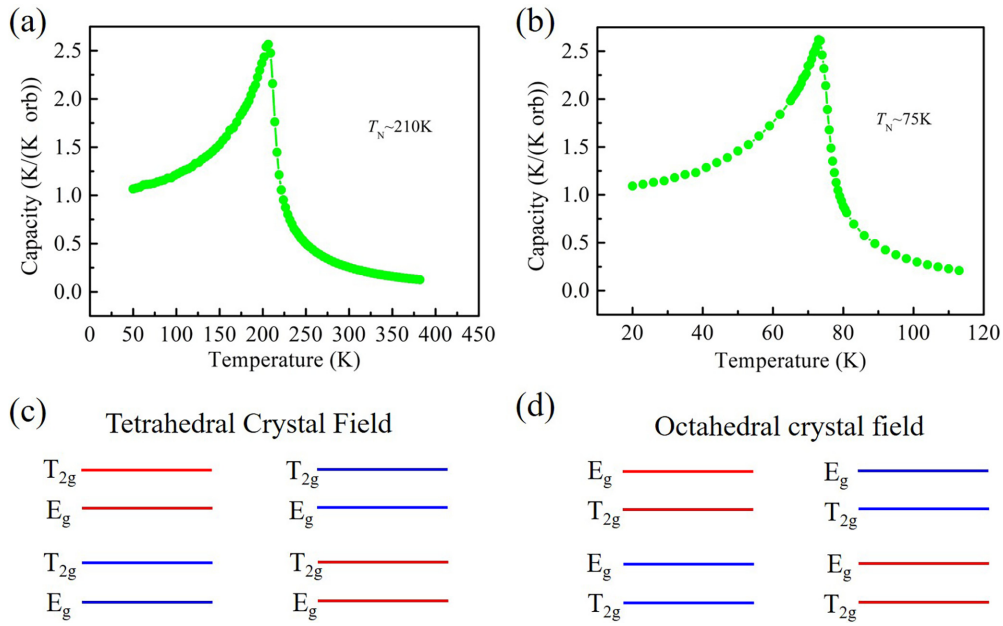


FIG. 4. The magnetic transition temperatures and schematic diagram of crystal field splitting of $M(CN)_2$. (a) and (b) are evolution of specific heat capacity with temperature of $Mn(CN)_2$ and $Co(CN)_2$, respectively. (c) and (d) are the splitting schematics of $d$ orbitals in tetrahedral and octahedral crystal fields, respectively. The magnetic transition temperatures are calculated under correlation interaction $U =$ 4 eV.

or $Co^{+2}$ with opposite magnetic moments are approximately equal, only the spins are opposite. Therefore, although both $Mn(CN)_2$ and $Co(CN)_2$ do not have crystal symmetry $T\tau$, they have symmetry $T\tau$ at the charge density level. We call the $T\tau$ quasisymmetry, which can make net magnetic moment zero.

Considering another case, in $Ti(CN)_2$, two $3d$ electrons of $Ti^{+2}$ ions fill exactly the low energy $E_g$ orbit, resulting in completely quenched orbital moments. $Ti(CN)_2$ is thus an insulator, and is also a Luttinger compensated magnetic material. It also has quasisymmetry $T\tau$, which is proved by our calculations. Unfortunately, the phonon spectrum of $Ti(CN)_2$ has imaginary frequencies, which makes $Ti(CN)_2$ unstable. If the $E_g$ orbital or $T_{2g}$ orbital is partially filled, the orbital moments of $d$ electrons will not be completely quenched and the materials should be metallic. By calculating $V(CN)_2$, $Cr(CN)_2$, $Fe(CN)_2$, and $Ni(CN)_2$, we find that the total magnetic moments of these magnetic materials is not exactly zero. For octahedral crystal field, the $3d$ orbits are also split into $E_g$ and $T_{2g}$ orbits, but the $E_g$ orbit is higher in energy than the $T_{2g}$ orbit as shown in Fig. 4(d). Then, the $d$ electrons must be 3, 5, and 8 to guarantee the completely quenched orbital moments for high-spin states, in addition to satisfying the last two of the above three points, so that the material could be a Luttinger compensated magnet. Similarly, our analysis results can be also generalized to the materials containing $4f$ atoms. In a word, the Luttinger compensated magnets need to satisfy two conditions: (i) The $d$ orbital electrons of magnetic ions fully fill the $e_g$ and $t_{2g}$ orbitals for tetrahedral and octahedral crystal fields, so that the corresponding magnetic materials have an equal number of valence electrons with opposite polarization, resulting in a total spin magnetic moment of zero; (ii) The magnetic ions are in a high-spin state to quench the orbital magnetic moment.

Luttinger compensated bipolarized magnetic semiconductors hold potential advantages for applications in spintronic devices. For example, since its conduction and valence bands exhibit opposite spin polarizations, the application of opposite gate voltages can modulate the distinct spin polarizations in $Co(CN)_2$ and $Mn(CN)_2$, enabling the switching of the current between "on" and "off" states. This corresponds to the realization of a spin field-effect transistor. Moreover, spin-polarized electrons can also be electrically injected into nonmagnetic semiconductors to achieve the transmission of spin information. Although both $Mn(CN)_2$ and $Co(CN)_2$ are Luttinger compensated bipolarized magnetic semiconductors, their Néel temperatures are below room temperature. Interestingly, the Néel temperature of $Mn(CN)_2$ can increase to 500 K under 2% compressive strain. Therefore, in the future, we need to find Luttinger compensated magnetic materials with feasible properties, such as the transition temperature above the room temperature, the energy gap being in the semiconductor range, and the materials being nontoxicity.

In summary, based on symmetry analysis and the first-principles electronic structure calculations, we propose a class of Luttinger compensated bipolarized magnetic materials with quasisymmetry $T\tau$, represented by $Mn(CN)_2$ and $Co(CN)_2$. The full compensation (or exactly zero total magnetic moments) arise from the completely quenched orbital magnetic moments, the insulativity of materials, and the subsequent requirement that the spin magnetic moments per unit cell must be integer Bohr magnetons by the Luttinger theorem. Considering that the Luttinger compensated magnetic materials take the advantages of both ferromagnetic spin splitting and antiferromagnetic zero total magnetic moments, our work not only enriches the classification of magnetic materials, but also provides possibilities for applications in electronic devices.

*Acknowledgments.* This work was financially supported by the National Key R&D Program of China (Grants No. 2024YFA1408601, No. 2024YFA1408603, and No. 2023YFA1406500), the National Natural Science Foundation of China (Grants No. 12434009, No. 12204533, No. 62476278, No. 92477205, and No. 5246116032), and the Research Funds of Renmin University of China (Grants No. 24XNKJ15 and No. 22XNKJ30).

P.-J.G. and H.-C.Y. contributed equally to this work.

*Data availability.* The data that support the findings of this article are not publicly available. The data are available from the authors upon reasonable request.

[1] S. A. Wolf, D. D. Awschalom, R. A. Buhrman, J. M. Daughton, S. von Molnar, M. L. Roukes, A. Y. Chtchelkanova, and D. M. Treger, Spintronics: A spin-based electronics vision for the future, Science **294**, 1488 (2001).

[2] A. H. MacDonald, P. Schiffer, and N. Samarth, Ferromagnetic semiconductors: Moving beyond (Ga,Mn)As, Nat. Mater. **4**, 195 (2005).

[3] T. Dietl and H. Ohno, Dilute ferromagnetic semiconductors: Physics and spintronic structures, Rev. Mod. Phys. **86**, 187 (2014).

[4] C. Gong and X. Zhang, Two-dimensional magnetic crystals and emergent heterostructure devices, Science **363**, eaav4450 (2019).

[5] T. Masaaki, Recent progress in ferromagnetic semiconductors and spintronics devices, Jpn. J. Appl. Phys. **60**, 010101 (2020).

[6] B. Huang, G. Clark, E. Navarro-Moratalla, D. R. Klein, R. Cheng, K. L. Seyler, D. Zhong, E. Schmidgall, M. A. McGuire, D. H. Cobden, W. Yao, D. Xiao, P. Jarillo-Herrero, and X. D. Xu, Layer-dependent ferromagnetism in a van der waals crystal down to the monolayer limit, Nature (London) **546**, 270 (2017).

[7] Z. W. Zhang, J. Z. Shang, C. Y. Jiang, A. Rasmita, W. B. Gao, and T. Yu, Direct photoluminescence probing of ferromagnetism in monolayer two-dimensional $CrBr_3$, Nano Lett. **19**, 3138 (2019).

[8] C. Gong, L. Li, Z. L. Li, H. W. Ji, A. Stern, Y. Xia, T. Cao, W. Bao, C. Z. Wang, Y. Wang, Z. Q. Qiu, R. J. Cava, S. G. Louie, J. Xia, and X. Zhang, Discovery of intrinsic ferromagnetism in two-dimensional van der waals crystals, Nature (London) **546**, 265 (2017).

[9] X. X. Li and J. L. Yang, $CrXTe_3$ (X = Si, Ge) nanosheets: Two dimensional intrinsic ferromagnetic semiconductors, J. Mater. Chem. C **2**, 7071 (2014).

[10] V. V. Kulish and W. Huang, Single-layer metal halides $MX_2$(X = Cl, Br, I): Stability and tunable magnetism from

first principles and Monte Carlo simulations, J. Mater. Chem. C **5**, 8734 (2017).
[11] J. Y. You, Z. Zhang, X. J. Dong, B. Gu, and G. Su, Two-dimensional magnetic semiconductors with room Curie temperatures, Phys. Rev. Res. **2**, 013002 (2020).
[12] L. Šmejkal, J. Sinova, and T. Jungwirth, Emerging research landscape of altermagnetism, Phys. Rev. X **12**, 040501 (2022).
[13] L. Šmejkal, J. Sinova, and T. Jungwirth, Beyond conventional ferromagnetism and antiferromagnetism: A phase with nonrelativistic spin and crystal rotation symmetry, Phys. Rev. X **12**, 031042 (2022).
[14] S. Hayami, Y. Yanagi, and H. Kusunose, Momentum-Dependent spin splitting by collinear antiferromagnetic ordering, J. Phys. Soc. Jpn. **88**, 123702 (2019).
[15] L. Šmejkal, R. González-Hernández, T. Jungwirth, and J. Sinova, Crystal time-reversal symmetry breaking and spontaneous Hall effect in collinear antiferromagnets, Sci. Adv. **6**, eaaz8809 (2020).
[16] L.-D. Yuan, Z. Wang, J.-W. Luo, E. I. Rashba, and A. Zunger, Giant momentum-dependent spin splitting in centrosymmetric low-*Z* antiferromagnets, Phys. Rev. B **102**, 014422 (2020).
[17] I. I. Mazin, K. Koepernik, M. D. Johannes, R. González-Hernández, and L. Šmejkal, Prediction of unconventional magnetism in doped $FeSb_2$, Proc. Natl. Acad. Sci. USA **118**, e2108924118 (2021).
[18] I. Mazin, Editorial: Altermagnetism—a new punch line of fundamental magnetism, Phys. Rev. X **12**, 040002 (2022).
[19] P.-J. Guo, Z.-X. Liu, and Z.-Y. Lu, Quantum anomalous Hall effect in collinear antiferromagnetism, npj Comput. Mater. **9**, 70 (2023).
[20] R. González-Hernández, L. Šmejkal, K. Výborný, Y. Yahagi, J. Sinova, T. c. v. Jungwirth, and J. Železný, Efficient electrical spin splitter based on nonrelativistic collinear antiferromagnetism, Phys. Rev. Lett. **126**, 127701 (2021).
[21] H. Bai, L. Han, X. Y. Feng, Y. J. Zhou, R. X. Su, Q. Wang, L. Y. Liao, W. X. Zhu, X. Z. Chen, F. Pan, X. L. Fan, and C. Song, Observation of spin splitting torque in a collinear antiferromagnet $RuO_2$, Phys. Rev. Lett. **128**, 197202 (2022).
[22] S. Karube, T. Tanaka, D. Sugawara, N. Kadoguchi, M. Kohda, and J. Nitta, Observation of spin-splitter torque in collinear antiferromagnetic $RuO_2$, Phys. Rev. Lett. **129**, 137201 (2022).
[23] A. Bose, N. J. Schreiber, R. Jain, D.-F. Shao, H. P. Nair, J. Sun, X. S. Zhang, D. A. Muller, E. Y. Tsymbal, D. G. Schlom, and D. C. Ralph, Tilted spin current generated by the collinear antiferromagnet ruthenium dioxide, Nat. Electron. **5**, 267 (2022).
[24] L. Šmejkal, A. B. Hellenes, R. González-Hernández, J. Sinova, and T. Jungwirth, Giant and tunneling magnetoresistance in unconventional collinear antiferromagnets with nonrelativistic spin-momentum coupling, Phys. Rev. X **12**, 011028 (2022).
[25] R.-W. Zhang, C. Cui, R. Li, J. Duan, L. Li, Z.-M. Yu, and Y. Yao, Predictable gate-field control of spin in altermagnets with spin-layer coupling, Phys. Rev. Lett. **133**, 056401 (2024).
[26] D.-F. Shao, S.-H. Zhang, M. Li, C.-B. Eom, and E. Tsymbal, Spin-neutral currents for spintronics, Nat. Commun. **12**, 7061 (2021).
[27] D. Zhu, Z.-Y. Zhuang, Z. Wu, and Z. Yan, Topological superconductivity in two-dimensional altermagnetic metals, Phys. Rev. B **108**, 184505 (2023).
[28] L. Šmejkal, A. H. MacDonald, J. Sinova, S. Nakatsuji, and T. Jungwirth, Anomalous Hall antiferromagnets, Nat. Rev. Mater. **7**, 482 (2022).
[29] Z. Feng, X. Zhou, L. Šmejkal, L. Wu, Z. Zhu, H. Guo, R. González-Hernández, X. Wang, H. Yan, P. Qin, X. Zhang, H. Wu, H. Chen, Z. Meng, L. Liu, Z. Xia, J. Sinova, T. Jungwirth, and Z. Liu, An anomalous Hall effect in altermagnetic ruthenium dioxide, Nat. Electron. **5**, 735 (2022).
[30] R. D. Gonzalez Betancourt, J. Zubáč, R. Gonzalez-Hernandez, K. Geishendorf, Z. Šobáň, G. Springholz, K. Olejník, L. Šmejkal, J. Sinova, T. Jungwirth, S. T. B. Goennenwein, A. Thomas, H. Reichlová, J. Železný, and D. Kriegner, Spontaneous anomalous Hall effect arising from an unconventional compensated magnetic phase in a semiconductor, Phys. Rev. Lett. **130**, 036702 (2023).
[31] X.-Y. Hou, H.-C. Yang, Z.-X. Liu, P.-J. Guo, and Z.-Y. Lu, Large intrinsic anomalous Hall effect in both $Nb_2FeB_2$ and $Ta_2FeB_2$ with collinear antiferromagnetism, Phys. Rev. B **107**, L161109 (2023).
[32] X. Zhou, W. Feng, X. Yang, G.-Y. Guo, and Y. Yao, Crystal chirality magneto-optical effects in collinear antiferromagnets, Phys. Rev. B **104**, 024401 (2021).
[33] X. Zhou, W. Feng, R.-W. Zhang, L. Šmejkal, J. Sinova, Y. Mokrousov, and Y. Yao, Crystal thermal transport in altermagnetic $RuO_2$, Phys. Rev. Lett. **132**, 056701 (2024).
[34] Y.-X. Li, Y. Liu, and C.-C. Liu, Creation and manipulation of higher-order topological states by altermagnets, Phys. Rev. B **109**, L201109 (2024).
[35] Y.-X. Li and C.-C. Liu, Majorana corner modes and tunable patterns in an altermagnet heterostructure, Phys. Rev. B **108**, 205410 (2023).
[36] P.-J. Guo, Y. Gu, Z.-F. Gao, and Z.-Y. Lu, Altermagnetic ferroelectric $LiFe_2F_6$ and spin-triplet excitonic insulator phase, arXiv:2312.13911.
[37] S. Qu, Z.-F. Gao, H. Sun, K. Liu, P.-J. Guo, and Z.-Y. Lu, Extremely strong spin-orbit coupling effect in light element altermagnetic materials, Front. Phys. **21**, 045203 (2025).
[38] C.-Y. Tan, Z.-F. Gao, H.-C. Yang, K. Liu, P.-J. Guo, and Z.-Y. Lu, Bipolarized Weyl semimetals and quantum crystal valley Hall effect in two-dimensional altermagnetic materials, arXiv:2406.16603.
[39] C.-Y. Tan, Z.-F. Gao, H.-C. Yang, Z.-X. Liu, K. Liu, P.-J. Guo, and Z.-Y. Lu, Crystal valley Hall effect, Phys. Rev. B **111**, 094411 (2025).
[40] Z. Xiao, J. Zhao, Y. Li, R. Shindou, and Z.-D. Song, Spin space groups: Full classification and applications, Phys. Rev. X **14**, 031037 (2024).
[41] X. Chen, J. Ren, Y. Zhu, Y. Yu, A. Zhang, P. Liu, J. Li, Y. Liu, C. Li, and Q. Liu, Enumeration and representation theory of spin space groups, Phys. Rev. X **14**, 031038 (2024).
[42] Z.-F. Gao, S. Qu, B.-C. Zeng, Y. Liu, J.-R. Wen, H. Sun, P.-J. Guo, and Z.-Y. Lu, AI-accelerated discovery of altermagnetic materials, Natl. Sci. Rev. **12**, nwaf066 (2025).
[43] J. M. Luttinger and J. C. Ward, Ground-state energy of a many-fermion system, Phys. Rev. **118**, 1417 (1960).
[44] J. M. Luttinger, Fermi surface and some simple equilibrium properties of a system of interacting fermions, Phys. Rev. **119**, 1153 (1960).
[45] H. van Leuken and R. A. de Groot, Half-metallic antiferromagnets, Phys. Rev. Lett. **74**, 1171 (1995).

[46] S. Wurmehl, H. C. Kandpal, G. H. Fecher, and C. Felser, Valence electron rules for prediction of half-metallic compensated-ferrimagnetic behavior of heusler compounds with complete spin polarization, J. Phys.: Condens. Matter **18**, 6171 (2006).

[47] T. Kawamura, K. Yoshimi, K. Hashimoto, A. Kobayashi, and T. Misawa, Compensated ferrimagnets with colossal spin splitting in organic compounds, Phys. Rev. Lett. **132**, 156502 (2024).

[48] L.-D. Yuan, A. B. Georgescu, and J. M. Rondinelli, Nonrelativistic spin splitting at the Brillouin zone center in compensated magnets, Phys. Rev. Lett. **133**, 216701 (2024).

[49] Y. Liu, S.-D. Guo, Y. Li, and C.-C. Liu, Two-dimensional fully compensated ferrimagnetism, Phys. Rev. Lett. **134**, 116703 (2025).

[50] G. Kresse and J. Furthmüller, Efficiency of *ab-initio* total energy calculations for metals and semiconductors using a plane-wave basis set, Comput. Mater. Sci. **6**, 15 (1996).

[51] P. E. Blöchl, Projector augmented-wave method, Phys. Rev. B **50**, 17953 (1994).

[52] J. P. Perdew, K. Burke, and M. Ernzerhof, Generalized gradient approximation made simple, Phys. Rev. Lett. **77**, 3865 (1996).

[53] V. I. Anisimov, J. Zaanen, and O. K. Andersen, Band theory and mott insulators: Hubbard U instead of stoner *I*, Phys. Rev. B **44**, 943 (1991).

[54] S. L. Dudarev, G. A. Botton, S. Y. Savrasov, C. J. Humphreys, and A. P. Sutton, Electron-energy-loss spectra and the structural stability of nickel oxide: An LSDA+U study, Phys. Rev. B **57**, 1505 (1998).

[55] L. Liu, X. Ren, J. H. Xie, B. Cheng, W. K. Liu, T. Y. An, H. W. Qin, and J. F. Hu, Magnetic switches via electric field in BN nanoribbons, Appl. Surf. Sci. **480**, 300 (2019).

[56] J. B. Goodenough, *Magnetism and the Chemical Bond* (Interscience Publishers, New York, 1963).